Inorganic Chemistry

COMMUNICATION

pubs.acs.org/IC

A Mild Liquid Reduction Route toward Uniform Blue-Emitting $EuCl_2$ Nanoprisms and Nanorods

Weili Jiang, Zuqiang Bian,* Chenming Hong, and Chunhui Huang

Beijing National Laboratory for Molecular Sciences, State Key Laboratory of Rare Earth Materials Chemistry and Applications, College of Chemistry and Molecular Engineering, Peking University, Beijing 100871, China

Supporting Information

ABSTRACT: In this work, for the first time, uniform blue-emitting $EuCl_2$ nanoprisms and nanorods were synthesized from $Eu(CCl_3COO)_3 \cdot 2H_2O$ [or $Eu(CH_3COO)_3 \cdot H_2O$] by a novel mild liquid reduction route, using acetamidine hydrochloride (or picolinamidine hydrochloride) as the reductant in oleylamine. The synthetic reaction even can take place under an atmosphere in the absence of inert gas at around 300 °C. The $EuCl_2$ nanoprism dispersion in *n*-hexane showed an intense blue emission when excited by UV light.

Uniform inorganic nanocrystals have aroused wide interests during the last 2 decades because of their shape- and size-dependent properties and self-assembly potential in devices and bioassays.[1] One of the most important categories is lanthanide compound nanocrystals with rich optical, electric, and magnetic properties caused by their special 4f electrons.[2] Despite a good deal of work focusing on the stable trivalent lanthanide compounds, such as oxides,[2b] fluorides,[2d−f,h] phosphates,[2a,c] and vanadates,[2g] the number of publications on divalent lanthanide compound nanocrystals (especially for Eu^{II} nanocrystals with potential as optomagnetic and luminescent materials) is still limited. Uniform Eu^{II} nanocrystals reported so far are mainly europium chalcogenides, EuX (X = O, S, Se).[3] In 2005−2006, the groups of Scholes[3a] and Gao[3b] synthesized uniform EuS nanocrystals by the thermal decomposition of $Eu(ddtc)_3(phen)$. Later, Hasegawa et al. prepared uniform $Eu_{1-x}Se$ nanoparticles by the thermal reduction of Eu^{3+} ion with organic ligands containing Se atoms.[3e] These nanomaterials show attractive semiconductive and magnetic properties. Hasegawa et al. also found special luminescent properties for small EuO[4] and EuS[5] nanocrystals.

Other common binary Eu^{II} compounds, europium dihalides EuX_2 (X = F, Cl, Br, I), have been studied since the 1930s.[6] Interesting magnetic properties were found consistently for EuX_2 (X = Cl, Br, I),[7] and tunable luminescence around 400−500 nm was also observed for europium dihalides, which originates from the d−f transition of Eu^{2+} sensitive to the environment.[8] However, few works have been reported on europium dihalide nanocrystals largely because of the difficulty in preparation caused by the instability of Eu^{2+} ions.[9] Recently, Mudring et al. prepared nanoscale EuF_2 from its bulk material via physical vapor deposition into ionic liquids.[10] Such a method was relatively complex and unsuitable for other europium dihalides.

Herein, we report the first synthesis of uniform $EuCl_2$ nanoprisms and nanorods, from $Eu(CCl_3COO)_3 \cdot 2H_2O$ [or $Eu(CH_3COO)_3 \cdot H_2O$] by a novel mild liquid reduction route, with acetamidine hydrochloride [AAM, or picolinamidine hydrochloride (PAM)] as the reductant in oleylamine (OM). Interestingly, the $EuCl_2$ nanoprisms dispersed in *n*-hexane exhibited intense blue emission under UV-light excitation.

In a typical synthesis, $Eu(CCl_3COO)_3 \cdot 2H_2O$ (0.30 mmol) and AAM (1.0 mmol) were mixed in OM (30 mmol). The mixture was stirred at about 40 °C until a clear, colorless solution formed. The solution was then heated rapidly to 300 °C, where it was maintained for 1 h under stirring. After cooling, ethanol (30 mL) was added to precipitate a gray-white product. The thus-obtained $EuCl_2$ nanoprisms were likely produced through the pathway described in Scheme 1. As is known, Eu^{3+} ions can be reduced to Eu^{2+} ions by ammonia.[11] Here, AAM was selected as the reductant precursor, which could decompose at about 300 °C to release ammonia.[12]

The powder X-ray diffraction (PXRD) pattern of the obtained nanoparticles is shown in Figure 1a (top) and is consistent with orthorhombic $EuCl_2$ (JCPDS card file, 73-0279; space group, *Pbnm*; a = 8.965 Å, b = 7.538 Å, and c = 4.511 Å), indicating formation of the target compound. Figure 1b shows the morphology of the product observed by transmission electron microscopy (TEM). The nanoparticles are uniform and appear to be in the shape of hexagonal nanoprisms with sides of about 17.7 ± 1.7 nm and a thickness of 20.5 ± 1.6 nm in length [Figure S1 in the Supporting Information (SI) and Figure 1b inset, indicated by arrows]. The high-resolution TEM (HRTEM) image in Figure 1c shows an interplanar spacing of 0.39 nm in the [210] direction. The fast Fourier transform (FFT) pattern of the lattice planes (inset in Figure 1c) reveals that the hexagonal prism is projected from the [001] direction. As observed from the HRTEM image, the nanoprsims are single-crystalline in the core domain and partially amorphous in the thin-shell region. The FFT pattern shows some bright diffraction spots superimposed on a diffuse halo, also suggesting a mixture of crystalline and amorphous phases coexisting for the $EuCl_2$ nanoprisms. As determined from the energy-dispersive X-ray (EDX) spectrum (Figure S2 in the SI), the nanoprisms contain the atoms of Eu, Cl, and O at a ratio of Eu:Cl:O = 1:1.59:0.5. These results suggest that a partial surface oxidization took place for the nanoprisms, with the formation of a partially amorphous shell onto the nanoprisms due to the insertion of O atoms into the surface layers of the nanoprisms. X-ray photoelectron spectroscopy (XPS; Figure S3 in the SI) analysis shows the clear presence of Eu^{2+} (128.23 and ∼134 eV) and Cl^-

Received: May 11, 2011
Published: June 23, 2011

Scheme 1. Formation Pathway of $EuCl_2$ Nanoprisms

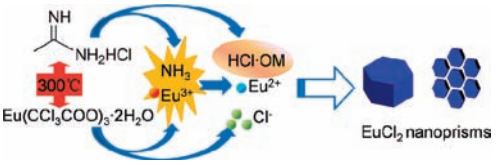

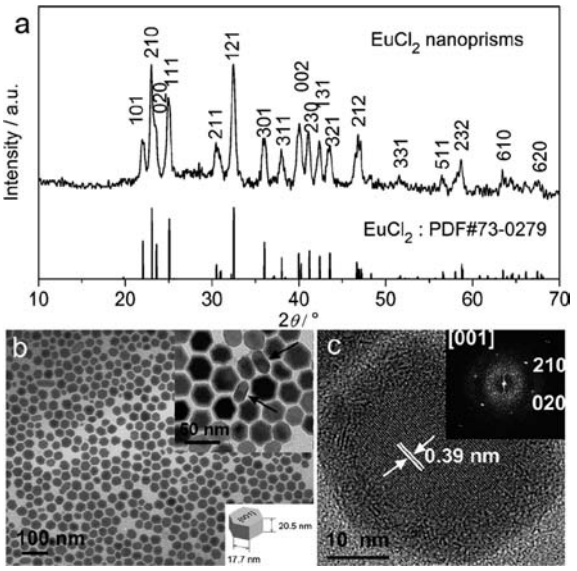

Figure 1. (a) PXRD pattern of $EuCl_2$ nanoprisms (top) and the JCPDS card file for $EuCl_2$ (bottom). (b) TEM images and a structural model of the nanoprisms. (c) HRTEM image and FFT pattern (inset) of the $EuCl_2$ nanoprisms.

(198.42 eV), although some surface Eu^{2+} ions have been oxidized to Eu^{3+} (~136 and 142.23 eV)[13] after the sample was exposed to air for a week. The observed strong band of O 1s (531.47 eV) again indicates that a doping of O atoms into the nanoprism lattices might occur to form a surface oxide layer due to air oxidation of the surface Eu^{2+} ions (Figure 1c).[3d,14] The Fourier transform infrared (FT-IR) spectrum of the nanoprisms (Figure S4 in the SI) proves the existence of OM ligands on the surfaces of the nanoprisms.

Control experiments have been carried out to reveal the key factors governing the selective formation of the $EuCl_2$ nanoparticles in this synthesis. Because the decomposition temperature (T_d) of AAM is 292 °C (Figure S5 in the SI), the reaction temperature is critical for synthesis of the $EuCl_2$ product (Figures S7 and S7 in the SI).

When the reaction was performed under a flow of N_2, the size of the product gets larger (Figure S8a in the SI). In the present synthesis, it was also found that the sole use of OM as the solvent could well control the growth of the nanoprisms because of its well surface capping by providing steric stabilization and preventing aggregation of the nanoparticles. When the inert solvent of octadecene (ODE) was introduced into the reaction media (i.e., the solvent composition was changed to OM:ODE = 1:1), less uniform $EuCl_2$ nanoprisms were obtained (Figure S8b in the SI), indicating that the use of ODE was ineffective at controlling the nanoparticle growth. Further, little precipitates formed when oleic acid (OA) was used as the cosurfactants (OM:OA = 1:1 or ODE:OA = 1:1) because it may be harmful to the generated ammonia.

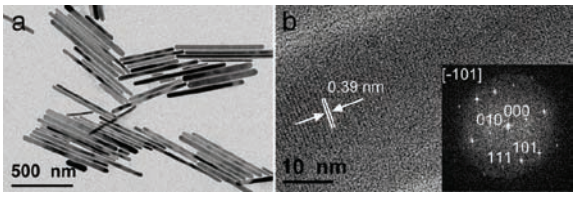

Figure 2. (a) TEM and (b) HRTEM (FFT pattern, inset) images of the $EuCl_2$ nanorods synthesized from AAM and $Eu(CH_3COO)_3 \cdot H_2O$.

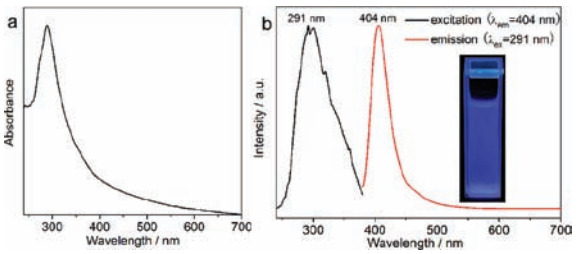

Figure 3. (a) UV−vis absorption and (b) excitation (λ_{em} = 404 nm) and emission (λ_{ex} = 291 nm) spectra of $EuCl_2$ nanoprisms dispersed in *n*-hexane at room temperature (0.4 g L^{-1}). Inset: Photograph of the suspension excited with a UV lamp at 365 nm.

Another reductant, PAM, was also synthesized to explore the reaction mechanism in OM at 300 °C under atmospheric conditions. As expected, similar $EuCl_2$ nanoprisms (Figures S9 and S10 in the SI) were produced, revealing that the amidine group is an important active species while the different substituent groups do not influence the reaction. However, if $Eu(CH_3COO)_3 \cdot H_2O$ was used as the Eu^{3+} precursor, long nanorods of $EuCl_2$ were synthesized when either AAM (Figures 2 and S10 in the SI) or PAM (Figures S9 and S10 in the SI) was used as the reductant. The nanorods have a size of about 180−800 nm × 34.4 ± 7.5 nm (Figure S11 in the SI), with an interplanar spacing of 0.39 nm in the [010] direction. Considering that $Eu(CCl_3COO)_3 \cdot 2H_2O$ has a lower T_d (250 °C; Figure S5 in the SI) than $Eu(CH_3COO)_3 \cdot H_2O$ (374 °C), the possible reason for the formation of differently shaped $EuCl_2$ nanoparticles is that the rapid decomposition of $Eu(CCl_3COO)_3 \cdot 2H_2O$ and the thus-released much more Cl^- species made the particles nucleate fast, suppressing the anisotropic growth of $EuCl_2$ and leading to a smaller size distribution.[1e]

Figure 3a shows the UV−vis absorption spectrum of the $EuCl_2$ nanoprisms dispersed in *n*-hexane. The wide absorption band at 288 nm is assigned to the $4f^7 \rightarrow 4f^6 5d^1$ dipole transition of Eu^{2+} ions.[15] The excitation spectrum (Figure 3b) is similar to the absorption spectrum with a peak value at 291 nm, attributed to the $4f^7 \rightarrow 4f^6 5d^1$ transition. Besides, there is a staircase structure superposed on the lower-energy band, peaking at 300, 318, 331, and 359 nm. The first three peaks can be attributed to the transitions from the ground state of $4f^7$ to the spin−orbit multiplets of $4f^6 5d^1$, while the last one is attributed to the transition from the ground state of the $4f^7$ configuration ($^8S_{7/2}$) to the lowest excited state ($^6P_{7/2}$).[16] When excited at 291 nm, the suspension exhibited bright luminescence centered at 404 nm (Figure 3b), a typical broad emission attributed to the $4f^6 5d^1 \rightarrow 4f^7$ transition of Eu^{2+}.[16,17] It is noticeable that no emission above 500 nm was detected, meaning that the Eu^{3+} ions were reduced almost completely. Luminescence decay of the nanoprisms (Figure S12 in the SI) was best described by a biexponential function [τ_1 = 35.3 ns (57.0%) and τ_2 = 181.7 ns

dx.doi.org/10.1021/ic200993w |*Inorg. Chem.* 2011, 50, 6862–6864

(43.0%)], indicating that there are two luminescent centers in the sample. The shorter component corresponds to the luminescence of surface Eu^{2+} ions in the amorphous layer with more defect state quenching. The longer one is attributed to emission from the core Eu^{2+} ions.

The $EuCl_2$ nanorods dispersed in *n*-hexane have an emission band centered at 380 nm (Figure S13 in the SI), showing a 24-nm blue shift compared with the emission of nanoprisms caused by the influenced 4f−5d transition. The photoluminescent quantum yield (Φ) is 7.3% for the nanoprism suspension and just 1.1% for the nanorods. The supposed reason is that the Eu^{2+}−Eu^{2+} concentration quenching is reduced efficiently in the nanoprisms that have smaller particle size and dense surface Eu^{2+} sites.[18]

Furthermore, to study the stability of the $EuCl_2$ nanoprisms after they were stored in air for several months, luminescent measurements were performed by tracking the characteristic Eu^{3+} ion emission at 613 nm (Figure S14 in the SI). It was observed that, under the same measurement conditions, the emission at 613 nm was quite faint compared with the band at 404 nm, implying that Eu^{3+} ions are significantly less and the nanoprisms are stable in air. The PXRD and TEM results in Figure S15 in the SI show that the sample keeps its morphology and composition even after 6 months in air.

In summary, a simple liquid reduction method for the preparation of uniform $EuCl_2$ nanoprisms and nanorods in long-chain high-boiling solvents was developed. Thermal decomposition of amidine hydrochloride (AAM or PAM) at 300 °C generated ammonia, which reduced the Eu^{III} precursor to $EuCl_2$, even in the presence of air. $EuCl_2$ nanoprisms or nanorods were obtained respectively by choosing $Eu(CCl_3COO)_3 \cdot 2H_2O$ or $Eu(CH_3COO)_3 \cdot H_2O$ as the Eu^{III} precursor. The reaction temperature and surfactant composition were proved to be important factors affecting the formation of the target products. Photophysical studies revealed that the $EuCl_2$ nanoprisms exhibit typical blue emission from an f−d electronic transition of Eu^{2+} ions with a high quantum yield of 7.3%. We expect that this work can promote the controlled synthesis of divalent rare-earth nanocrystals and their new optical and biomedical applications.

■ ASSOCIATED CONTENT

Supporting Information. Additional characterization of $EuCl_2$ particles and precursors. This material is available free of charge via the Internet at http://pubs.acs.org.

■ AUTHOR INFORMATION

Corresponding Author

*E-mail: bianzq@pku.edu.cn. Tel: (+86)10-6275-3544. Fax: (+86)10-6275-7156.

■ ACKNOWLEDGMENT

This work is supported by the National Basic Research Program (Grant 2011CB9333200) and the National Natural Science Foundation of China (Grants 90922004, 20821091, and 20971006). We thank Prof. Y. W. Zhang and L. D. Sun (Peking University, Beijing, China) for their helpful suggestions.

■ REFERENCES

(1) (a) Murray, C. B.; Norris, D. J.; Bawendi, M. G. *J. Am. Chem. Soc.* **1993**, *115*, 8706–8715. (b) Ahmadi, T. S.; Wang, Z. L.; Green, T. C.; Henglein, A.; El Sayed, M. A. *Science* **1996**, *272*, 1924–1926. (c) Bruchez, M.; Moronne, M.; Gin, P.; Weiss, S.; Alivisatos, A. P. *Science* **1998**, *281*, 2013–2016. (d) Rabani, E.; Reichman, D. R.; Geissler, P. L.; Brus, L. E. *Nature* **2003**, *426*, 271–274. (e) Yin, Y.; Alivisatos, A. P. *Nature* **2005**, *437*, 664–670. (f) Wang, X.; Zhuang, J.; Peng, Q.; Li, Y. D. *Nature* **2005**, *437*, 121–124. (g) Medintz, I. L.; Uyeda, H. T.; Goldman, E. R.; Mattoussi, H. *Nat. Mater.* **2005**, *4*, 435–446. (h) Nie, Z. H.; Petukhova, A.; Kumacheva, E. *Nat. Nanotechnol.* **2010**, *5*, 15–25.

(2) (a) Kompe, K.; Borchert, H.; Storz, J.; Lobo, A.; Adam, S.; Moller, T.; Haase, M. *Angew. Chem., Int. Ed.* **2003**, *42*, 5513–5516. (b) Si, R.; Zhang, Y. W.; You, L. P.; Yan, C. H. *Angew. Chem., Int. Ed.* **2005**, *44*, 3256–3260. (c) Huo, Z. Y.; Chen, C.; Chu, D.; Li, H. H.; Li, Y. D. *Chem.—Eur. J.* **2007**, *13*, 7708–7714. (d) Sun, X.; Zhang, Y. W.; Du, Y. P.; Yan, Z. G.; Si, R.; You, L. P.; Yan, C. H. *Chem.—Eur. J.* **2007**, *13*, 2320–2332. (e) Boyer, J. C.; Cuccia, L. A.; Capobianco, J. A. *Nano Lett.* **2007**, *7*, 847–852. (f) Chen, Z. G.; Chen, H. L.; Hu, H.; Yu, M. X.; Li, F. Y.; Zhang, Q.; Zhou, Z. G.; Yi, T.; Huang, C. H. *J. Am. Chem. Soc.* **2008**, *130*, 3023–3029. (g) Wang, F.; Xue, X. J.; Liu, X. G. *Angew. Chem., Int. Ed.* **2008**, *47*, 906–909. (h) Wang, F.; Han, Y.; Lim, C. S.; Lu, Y. H.; Wang, J.; Xu, J.; Chen, H. Y.; Zhang, C.; Hong, M. H.; Liu, X. G. *Nature* **2010**, *463*, 1061–1065.

(3) (a) Mirkovic, T.; Hines, M. A.; Nair, P. S.; Scholes, G. D. *Chem. Mater.* **2005**, *17*, 3451–3456. (b) Zhao, F.; Sun, H. L.; Su, G.; Gao, S. *Small* **2006**, *2*, 244–248. (c) Regulacio, M. D.; Bussmann, K.; Lewis, B.; Stoll, S. L. *J. Am. Chem. Soc.* **2006**, *128*, 11173–11179. (d) Bierman, M. J.; Van Heuvelen, K. M.; Schmeisser, D.; Brunold, T. C.; Jin, S. *Adv. Mater.* **2007**, *19*, 2677–2681. (e) Hasegawa, Y.; Adachi, T. A.; Tanaka, A.; Afzaal, M.; O'Brien, P.; Doi, T.; Hinatsu, Y.; Fujita, K.; Tanaka, K.; Kawai, T. *J. Am. Chem. Soc.* **2008**, *130*, 5710–5715. (f) Selinsky, R. S.; Han, J. H.; Perez, E. A. M.; Guzei, I. A.; Jin, S. *J. Am. Chem. Soc.* **2010**, *132*, 15997–16005. (g) Tanaka, A.; Kamikubo, H.; Doi, Y.; Hinatsu, Y.; Kataoka, M.; Kawai, T.; Hasegawa, Y. *Chem. Mater.* **2010**, *22*, 1776–1781.

(4) Hasegawa, Y.; Thongchant, S.; Wada, Y.; Tanaka, H.; Kawai, T.; Sakata, T.; Mori, H.; Yanagida, S. *Angew. Chem., Int. Ed.* **2002**, *41*, 2073–2075.

(5) Hasegawa, Y.; Okada, Y.; Kataoka, T.; Sakata, T.; Mori, H.; Wada, Y. *J. Phys. Chem. B* **2006**, *110*, 9008–9011.

(6) (a) Klemm, W. *Z. Anorg. Allg. Chem.* **1929**, *184*, 345–351. (b) Jantsch, G.; Skalla, N.; Grubitsch, H. *Z. Anorg. Allg. Chem.* **1933**, *216*, 75–79.

(7) Sanchez, J. P.; Friedt, J. M.; Barnighausen, H.; Vanduyneveldt, A. J. *Inorg. Chem.* **1985**, *24*, 408–415.

(8) (a) Dorenbos, P. *J. Lumin.* **2003**, *104*, 239–260. (b) Kobayashi, T.; Sekine, T.; Hirosaki, N. *Opt. Mater.* **2009**, *31*, 886–888.

(9) Song, Y. H.; You, H. P.; Yang, M.; Zheng, Y. H.; Liu, K.; Jia, G.; Huang, Y. J.; Zhang, L. H.; Zhang, H. J. *Inorg. Chem.* **2010**, *49*, 1674–1678.

(10) von Prondzinski, N.; Cybinska, J.; Mudring, A. V. *Chem. Commun.* **2010**, *46*, 4393–4395.

(11) Dekock, C. W.; Radtke, D. D. *J. Inorg. Nucl. Chem.* **1970**, *32*, 3687–3688.

(12) Shriner, R. L.; Neumann, F. W. *Chem. Rev.* **1944**, *35*, 351–425.

(13) Lu, D. Y.; Sugano, M.; Sun, X. Y.; Su, W. H. *Appl. Surf. Sci.* **2005**, *242*, 318–325.

(14) Zhao, F.; Sun, H. L.; Gao, S.; Su, G. *J. Mater. Chem.* **2005**, *15*, 4209–4214.

(15) (a) Freiser, M. J.; Methfess, S.; Holtzber, F. *J. Appl. Phys.* **1968**, *39*, 900–902. (b) Thongchant, S.; Hasegawa, Y.; Wada, Y.; Yanagida, S. *J. Phys. Chem. B* **2003**, *107*, 2193–2196.

(16) Kumar, V. R.; Narasimhulu, K. V.; Gopal, N. O.; Rao, J. L.; Chakradhar, R. P. S. *Physica B* **2004**, *348*, 446–453.

(17) Dorenbos, P. *J. Phys: Condens. Matter* **2003**, *15*, 2645–2665.

(18) Du, Y. P.; Zhang, Y. W.; Yan, Z. G.; Sun, L. D.; Yan, C. H. *J. Am. Chem. Soc.* **2009**, *131*, 16364–16365.